

# Double-Torsion Testing a 3Y-TZP Ceramic

J. Chevalier, M. Saadaoui, C. Olagnon & G. Fantozzi

INSA-GEMPPM, URA 341, 20 Avenue A. Einstein, 69621 Villeurbanne Cedex, France

(Received 10 January 1995; accepted 27 March 1995)

**Abstract:** Double torsion tests were performed to study subcritical crack growth of a 3Y-TZP ceramic. A significant variation of stress intensity factor  $K_I$  with crack length was observed. In order to take into account this variation a correction factor is introduced into the well-known analytical expression of stress intensity factor in mode I. This has enabled us to obtain accurate crack growth parameters i.e. an accurate measurement of (i) the three propagation stages of the subcritical crack growth and (ii) a threshold value equal to  $K_{I0} = 3.5 \text{ MPa}\sqrt{\text{m}}$ . Analytical expression of  $K_I$  based on a compliance analysis was shown to be unsatisfactory for slow crack growth analysis because of the influence of the unbroken ligament on the compressive side arising from the curved crack front.

## 1 INTRODUCTION

The time-dependent slow propagation of pre-existing cracks is one of the most important failure mechanisms of brittle materials, in particular ceramics, under long-term loading. Thus a detailed and precise understanding of this mechanism and eventually a corresponding quantitative analysis is necessary to predict life-time of ceramics accurately. The technique of double-torsion (DT) proposed by Kies and Clark<sup>1</sup> has received considerable attention as a direct method to determine toughness and subcritical crack growth (SCG) laws of ceramics, due to its simple geometry and the possibility of conducting extensive stable crack propagation in a wide range of velocities under constant loading or in a stress-relaxation mode.<sup>2–4</sup> Studies based on a compliance analysis<sup>5</sup> show that the stress intensity factor is independent of the crack length. Therefore, the DT test theoretically offers a significant advantage in comparison with other methods.

However, recently the authenticity of the test has been questioned.<sup>6</sup> The most important aspect was the effective constancy of the stress intensity factor ( $K_I$ ) over the specimen length. Indeed, the non-uniform stress distribution across the specimen thickness leads to a curved crack front,<sup>5</sup> while analytical calculation of  $K_I$  assumes a straight front. Several investigators have shown a relatively strong dependence of  $K_I$  on crack length. Multiple

relaxation tests performed on different polycrystalline ceramics present a shift to lower values of  $K_I$  as the initial crack length of the test increases, indicating an increase in the  $K_I$  value<sup>4</sup> with crack length during SCG tests.

Experiments on a soda-lime glass have shown a range of crack lengths where the stress intensity factor was constant.<sup>4</sup> Therefore this dependence of  $K_I$  on the crack length in polycrystalline materials has been attributed to the interaction of the crack with the microstructure.<sup>4</sup> At the same time the said dependence has also been argued as the consequence of a change in the compliance formula.<sup>7,8</sup> We believe that the unbroken ligament on the compressive side of the specimen due to the curved crack front may have a significant role and this has to be taken into consideration when determining the stress intensity factor.

The variation of  $K_I$  with the crack length has been studied using a finite element stress analysis proposed by Trantina,<sup>9</sup> and has been shown to depend greatly on the profile of the crack front. Corrections have also been proposed which considered the influence of the curved crack front on the determination of crack velocity.<sup>6,10,11</sup> However, these studies failed to account for the variation of  $K_I$  with crack length.

In the present investigation, a simple way of obtaining accurate slow crack growth parameters is proposed, keeping in mind the variation of  $K_I$

with crack length. It is well known that slow crack velocities are directly related to stress intensity factor at the crack tip in ceramics. Therefore, slow crack growth tests have been performed to study the influence of crack extension on crack velocities, and thence on  $K_I$ . Possible parameters which might be responsible for the observed variation of  $K_I$  will be discussed.

## 2 THEORETICAL BACKGROUND

A schematic view of the double-torsion specimen is shown in Fig. 1. The determination of  $K_I$  is based on a compliance analysis.<sup>5</sup> The first assumption (i) is that compliance  $C$ , given as the ratio of load-point displacement to the load, varies linearly with crack length  $a$ :

$$C = Ba + D \quad (1)$$

with  $B$  and  $D$  constant, dependent on the material properties.

The driving force for failure,  $G$ , is related to the applied load  $P$  and to the variation of compliance in the following expression:

$$G = \left( \frac{P^2}{2} \right) \left( \frac{\partial C}{\partial A} \right)_P \quad (2)$$

where  $\partial A$  is the increment of crack surface area with crack extension.<sup>5</sup>

Thus, following the assumption (i), eqn (2) becomes:

$$G = \frac{P^2 B}{2 \left( \frac{\partial C}{\partial a} \right)_P} \quad (3)$$

A second assumption (ii) leads to a simple expression for  $G$  (eqn (4)) where  $\partial A / \partial a$  corresponds to the thickness,  $T$ , of the specimen (this implies that the crack front is invariant with crack extension, and passes through the specimen thickness).

Thus eqn (3) can be rewritten as:

$$G = \frac{P^2 B}{2T} \quad (4)$$

Considering (iii) that the failure occurs in mode I, one can calculate  $K_I$  with the following expression:

$$K_I = \sqrt{2\mu(1+\nu)G} \quad (5)$$

where  $\nu$  is the Poisson's Ratio, and  $\mu$  the elastic shear modulus.

Theoretical analysis of the compliance of the DT specimen<sup>2</sup> also gives:

$$B = \left[ \frac{3Wm^2}{\mu WT^3 \Psi(T/W)} \right] \quad (6)$$

where  $W$  and  $Wm$  are the width of the specimen

and the moment arm, and  $\Psi(T/W)$  is a calibrating factor.<sup>4</sup> Then, the expression for  $K_I$  finally becomes:

$$K_I = HP \quad (7)$$

$$\text{with } H = \frac{Wm}{T^2} \left[ \frac{3(1+\nu)}{\Psi(T/W)W} \right]^{1/2} \quad (8)$$

We must note that the analytical stress intensity factor is therefore independent of the crack length. However, a number of assumptions are involved in this analysis and these will be discussed in detail later (see Section 5).

## 3 EXPERIMENTAL PROCEDURE

### 3.1 Material

The material studied in this work was an yttria-stabilized zirconia (3Y-TZP) sintered at 1450°C. A density of 6.06 g/cm<sup>3</sup> was measured by the Archimedes method and the average grain size was 0.58  $\mu$ m. 3Y-TZP has a homogeneous fine-grained tetragonal microstructure and thus can be considered as a model material for brittle polycrystalline ceramics. At the same time it exhibits a steeply rising R-Curve over few microns (~10  $\mu$ m), and a subsequent plateau toughness.<sup>12,13</sup> Therefore, the DT study in the present investigation using specimens containing large cracks was not perturbed by rising toughness.

### 3.2 Specimen geometry

The geometry of the DT specimen is shown in Fig. 1. No groove was machined on the tensile side in order to avoid any residual stress intensity factor.<sup>4</sup> The tensile surface was polished down to 1  $\mu$ m in order to observe the crack with a precision of  $\pm 2$   $\mu$ m. The notch of dimension: length  $a_0 = 10$  mm and root  $\rho = 0.1$  mm was machined with a diamond saw. Subsequent pre-cracking induced a sharp 'natural' crack of length of ~13 mm in each test specimen. A good alignment in the jig, associated

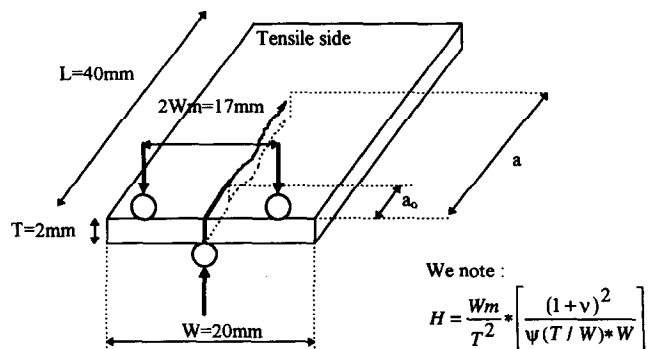


Fig. 1. Double-torsion specimen and loading configuration.

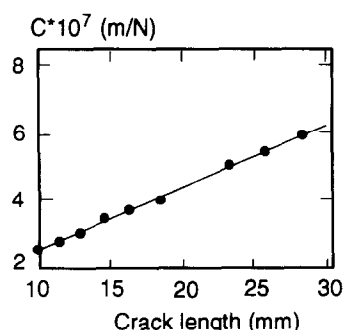


Fig. 2. Compliance  $C$  versus crack length  $a$ .

with a good control of the specimen parallelism, allowed straight propagation through the specimen to be achieved.

### 3.3 Testing methods

The experimental work consisted of constant loading and relaxation tests. In constant loading tests, specimens were subjected to static loads for different durations. The crack speed in each case was calculated as a ratio of crack increment to the loading time. SCG laws were recorded in the graphical form of the well-known ( $V$ - $K_I$ ) relation. In the relaxation tests the pre-cracked specimens were subjected to fast loading, followed by subsequent stopping of the crosshead at certain load value. Hence the crack propagation induced a load relaxation. The load versus time curve allowed the determination of the  $V$ - $K_I$  curve.<sup>5</sup>

## 4 EXPERIMENTAL RESULTS

### 4.1 Compliance analysis

In the range of crack lengths investigated (10–30 mm), the variation of the compliance  $C(a)$  was measured (Fig. 2). It is to be noted that in the present range of crack lengths  $C(a)$  is defined as a straight line that has been fitted by a linear regression

analysis using eqn (1). This resulted in values of  $B = 1.8 \times 10^{-5} \text{ N}^{-1}$  and  $D = 5.9 \times 10^{-8} \text{ mN}^{-1}$ . Calculation of the theoretical value of  $B$  ( $B_{th}$ ) from eqn (6) leads to:  $B_{th} = 2.0 \times 10^{-5} \text{ N}^{-1}$ . In the present study, possible changes in  $K_I$  with crack length therefore cannot be attributed to a change in compliance formulation, and this is relevant to assumption (i) (see Section 2).

### 4.2 Constant loading test

Constant loading tests were performed in order to investigate the relationship between crack length and crack velocity during subcritical crack extension in the linear region of compliance. For this purpose, a unique specimen was loaded alternatively by three loads (100 N, 105 N and 110 N) and crack velocity  $V$  was recorded as a function of crack length for each load. The results are presented in a  $\log(V)$  versus  $\log(a/a_0)$  plot (full symbols in Fig. 3). It appears that crack velocity increases with crack length for the three applied loads. The experimental results define three parallel straight lines.

Therefore, in the range of crack velocities investigated ( $10^{-9}$ – $10^{-5}$  m/s), and for a given applied load, the velocity  $V$  appears to be linked to the crack length by:

$$V = F(P)(a/a_0)^m \quad (9)$$

where  $a_0$  is the notch length,  $F(P)$  depends on the applied load and  $m$  appears to be independent of  $P$ .

We therefore defined a corrected velocity,  $V_{corr}$ , which is a function only of the applied load  $P$ , and is independent of the crack length.  $V_{corr}$  is related to  $V$  by:

$$V_{corr} = V(a_0/a)^m \quad (10)$$

### 4.3 Multi-relaxation test

In order to investigate the relationship between  $P$  and  $V_{corr}$ , multi-relaxation tests were performed on a single specimen for crack velocities in the range of  $10^{-7}$ – $10^{-5}$  m/s.

The results are presented in the form of  $\log(V)$  or  $\log(V_{corr})$  as a function of  $\log(P)$  in Fig. 4. The effect of crack length is obvious from the shifting of  $\log(V)$  vs  $\log(P)$  curves, although all of them show similar slopes. The increase of initial crack length in the relaxation test results in a shift to lower values of  $P$ , due to the influence of crack extension on  $K_I$ . Interestingly, the plot of  $\log(V_{corr})$  vs  $\log(P)$  does not present this shift, as the effect of crack length is now being taken into account. Note that

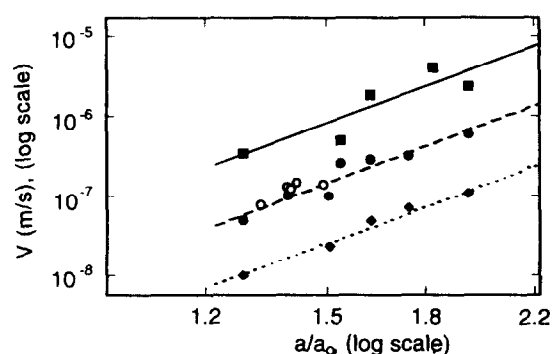


Fig. 3. Crack kinetic versus ratio of crack length to notch length for three applied loads. ■:  $P = 110$  N, ●:  $P = 105$  N, ♦:  $P = 100$  N, with  $a_0 = 10$  mm, ○:  $P = 105$  N, after renotching ( $a_0 = 21$  mm).

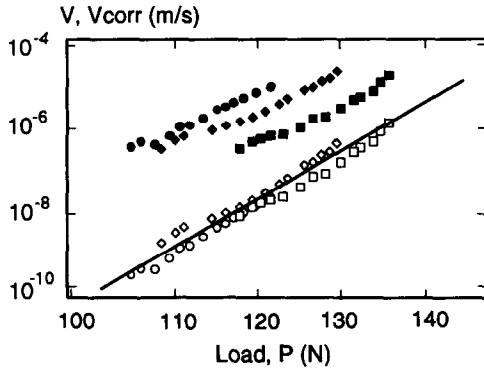


Fig. 4.  $V$  (full symbols) and  $V_{\text{corr}}$  (empty symbols) versus  $P$  for three successive relaxations on the same sample. ■ and □: Final crack length:  $a_f = 15.9$  mm, ♦ and ◇: Final crack length:  $a_f = 20.0$  mm, ● and ○: Final crack length:  $a_f = 27.2$  mm.

the slope of  $\log(V_{\text{corr}})$  vs  $\log(P)$  is different from those of the  $\log(V)$  vs  $\log(P)$  curves.

$V_{\text{corr}}$  can therefore be expressed as a function of  $P$  by:

$$V_{\text{corr}} = L(P)^k \quad (11)^*$$

#### 4.4 Correction factor for $K_I$

Combining eqns (10) and (11) gives:

$$V = LP^k \left( \frac{a}{a_0} \right)^m \quad (12)$$

Under the assumptions that (i) both the relaxation tests and the constant loading tests were performed in the first stage of the subcritical crack propagation law (crack velocity typically less than  $10^{-4}$  m/s), that is to say for velocities given by the power law relationship:<sup>14</sup>

$$V = AK_I^n \quad (13)$$

and (ii) the stress intensity factor is related to  $P$  and  $a$  by an empirical relationship of the form:

$$K_I = HP \left( \frac{a}{a_0} \right)^x \quad (14)^\dagger$$

Replacing the value of  $K_I$  from eqn (14) in (13) and comparing (14) with (12), we have:

\*It is to be noted that the calculation of  $V_{\text{corr}}$  during the relaxation requires the knowledge of crack length at each time of the test, which cannot directly be measured. Crack length can be calculated, by means of the following expression:

$$y = C_{\text{ste}} = C(a)P = C(a_f)P_f \quad (1b)$$

where  $y$  is the displacement (constant) during the relaxation test, and  $a_f$ ,  $P_f$  are, respectively, crack length and load at the end of the test.

Inserting eqn (1) in (1b), one can easily obtain:

$$a = \frac{\left( \frac{P_f(Ba_f + D)}{P} - D \right)}{B} \quad (2b)$$

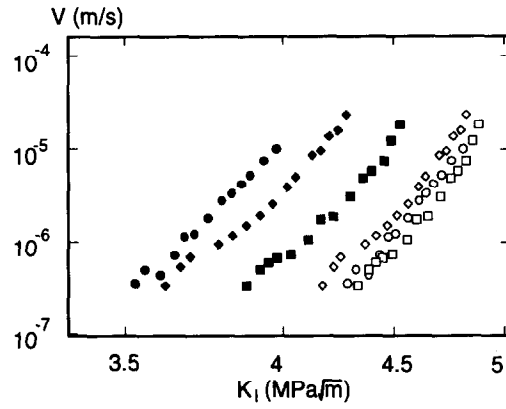


Fig. 5.  $V$ - $K_I$  graph resulting from the three relaxation tests with (empty symbols) and without (full symbols) correction. ■ and □: Final crack length:  $a_f = 15.9$  mm, ♦ and ◇: Final crack length:  $a_f = 20.0$  mm, ● and ○: Final crack length:  $a_f = 27.2$  mm.

$$n = k \quad \text{and} \quad x = m/n$$

Thus eqn (14) can be rewritten in the form:

$$K_I = HP \left( \frac{a}{a_0} \right)^{m/k} \quad (14b)$$

Hence  $K_I$  can be conveniently calculated from constant loading and multi-relaxation tests.

#### 4.5 Application

In the present section we will estimate values of  $m$  and  $k$  of eqn (14b). These values can be easily obtained using Figs 3 and 4, resulting in  $k = 32$  and  $m = 6$ . Therefore, the stress intensity factor is correctly given by:

$$K_I = HP \left( \frac{a}{a_0} \right)^{6/32} \quad (14c)$$

Figure 5 shows the results of the relaxation tests in the form of two sets of  $(\log V)$  vs  $(\log K_I)$  plots. The usual values of  $K_I$  (eqn (7)) are used in the case of first set (full symbols), whereas the second set (empty symbols) of results is plotted using the corrected values of  $K_I$  from eqn (14c). Poor reproducibility is observed in the resulting  $V$ - $K_I$  curves using the  $K_I$  value from eqn (7). On the contrary, we can have a single curve representing the  $V$ - $K_I$  relation using the other set of results where the change in  $K_I$  as a function of crack length was taken into account in the form of corrected values of  $K_I$ , defined in eqn (14c). It is clear

†The expression of  $K_I$  in the form of eqn (14) implies that eqn (7) is still valid for  $a = a_0$ . This hypothesis seems to be realistic because the notch defines an approximately straight crack front through the thickness, and the specimen in this case really consists of two independent beams. This assumption will be addressed later (see Section 5).

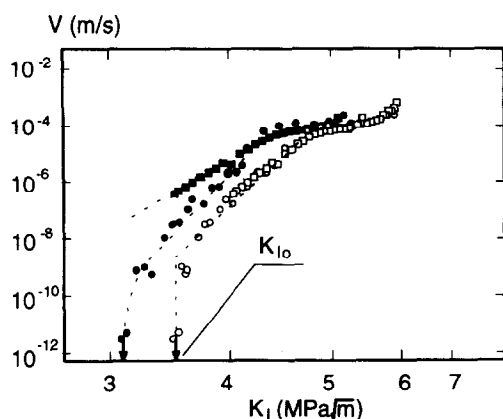


Fig. 6. Complete  $V$ - $K_I$  curves on 3Y-TZP. ■: Relaxation method, no correction. □: Relaxation method, with correction of  $K_I$ . ●: Constant load technique, no correction. ○: Constant load technique, with correction.

Table 1. Determination of crack growth parameters of the 3Y-TZP ceramic with and without correction

Method	$n$	$A$	$K_{I0}$ (MPa $\sqrt{m}$ )
Relaxation, no correction	21	$1.4 \times 10^{-18}$	$\approx 3.1$
Constant load, no correction	35.5	$7.5 \times 10^{-28}$	
Relaxation, corrected	31.5	$1.8 \times 10^{-26}$	3.5
Constant load, corrected	31.5	$1.8 \times 10^{-26}$	

that the correction leads to a much better reproducibility.

Additional stress relaxation and constant loading tests were performed at higher loads in order to determine the complete  $V$ - $K_I$  curve of the material, and the presence of a threshold  $K_{I0}$  was investigated with the constant load technique at low stress levels.

The 'classical'  $V$ - $K_I$  curves (using  $K_I$  values from eqn (7)) and the 'corrected'  $V$ - $K_I$  curves (using  $K_I$  values from eqn (14c)) are presented in Fig. 6. It is evident that the discrepancies involving the 'classical' curves can be conveniently taken into account in the case of 'corrected' curves owing to their good reproducibility at all the values of crack length. The presence of a threshold  $K_{I0}$  is also more pronounced in the later results. The measured crack

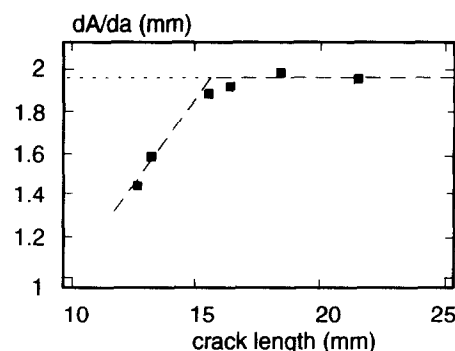


Fig. 8.  $\partial A/\partial a$  versus crack length  $a$ .

growth parameters ( $A$  and  $n$  in the first stage of slow crack growth,  $K_{I0}$ ) listed in Table 1 appear to be significantly different with and without correction. Thus one should be careful in choosing a value of  $K_I$  from eqn (7) when predicting the life-time of ceramics, and the choice of eqn (14) seems to be more appropriate.

## 5 DISCUSSION

So far we have shown that the classical expression of  $K_I$  (eqn (7)) is far from accurate as  $K_I$  is significantly dependent on crack length, accordingly a more precise estimation is obtained by means of eqn (14).

The observed increase of  $K_I$  was firstly thought to be due to a decrease of  $\partial A/\partial a$  with crack extension (non-verification of assumption (ii) in Section 2). Investigating this aspect further, a specimen was broken after several subcritical crack extension tests, and the fractured surface was analyzed using scanning electron microscopy. Figure 7 shows the schematic evolution of the crack profile from  $a = 10$  mm to  $a = 21$  mm. After an initial evolution of the crack geometry from 10 mm to 13–15 mm, the shape of the crack front remains unchanged during propagation.  $\partial A/\partial a$  has been calculated as the ratio of increment of crack surface area to the increase in crack length and its variation as a function of  $a$  is presented in Fig. 8. After an initial increase corresponding to the pre-cracking,  $\partial A/\partial a$  is constant over the present range of crack

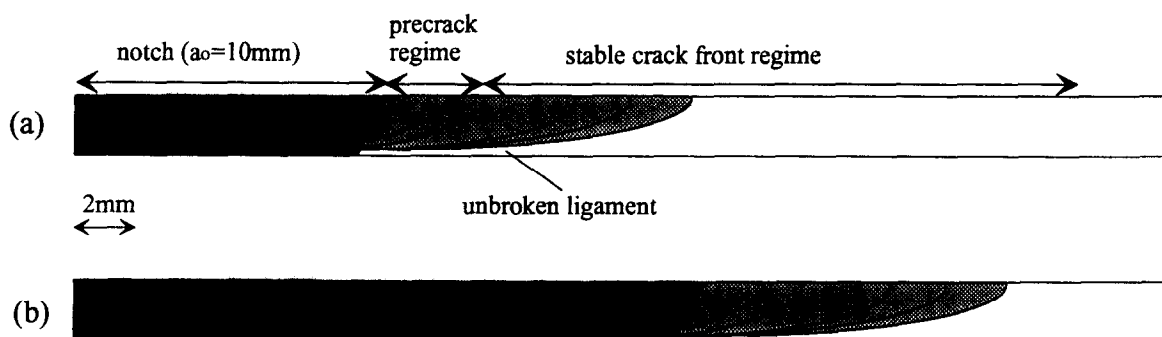


Fig. 7. Evolution of the crack front with crack extension. (a): notch length 10 mm, (b) notch length 21 mm.

lengths. The increase of  $K_I$  with crack extension cannot therefore be due to a decrease of  $\partial A/\partial a$ .

In a further argument we note that theoretical analysis of the DT specimen considers a straight crack front over the thickness, while obviously this is not valid in the experimental case. Therefore  $K_I$  must locally vary along the crack front. This has been quantified by Pollet and Burns,<sup>11</sup> who have introduced a calibration function  $\phi$  on crack velocities. True velocities ( $V$ ) were related to the experimentally measured crack velocities on the tensile surface by:

$$V = \phi V_{\text{measured}} \quad (15)$$

For a constant crack front geometry, as is the case in the present study,  $\phi$  is constant, which implies that the true velocity is proportional to measured crack velocity for a given applied load. Since  $\phi$  is constant, the observed variations of measured crack velocities with crack length cannot be corrected with the help of the so-called calibration function  $\phi$ . The value of  $\phi$  has been calculated for our crack front geometry, and leads to a correction factor value of 0.9 on crack velocities, independent of crack length. It therefore does not imply a significant change in the  $V$ - $K_I$  law for the present material. It is also to be noted that other similar corrections proposed in the literature<sup>6,10</sup> on crack velocities do not lead to more optimistic results.

To investigate the role of the unbroken ligament on the compressive side of the specimen, further renotching and subsequent constant loading experiments at 105 N were conducted on the sample previously used in constant loading tests (Section 4.2). The specimen was first renotched ( $a_0 = 21$  mm), and subsequently pre-cracked ( $a = 24$  mm), and this ensured identical configuration of the crack front previously obtained for the constant loading test in Section 4.2 (Fig. 7). Note that this renotching induces a decrease of the unbroken ligament area. It was interesting to note that, presently ( $a_0 = 21$  mm,  $a = 24$  mm), the crack velocity strongly decreased compared to the earlier case ( $a_0 = 10$  mm,  $a = 20$  mm). However, the present crack velocity was observed to be similar to the velocity obtained with  $a_0 = 10$  mm and  $a = 13$  mm. Thus the significant controlling factor for the variation of crack velocity is not the individual values of either  $a$  or  $a_0$  but rather the relation between  $a$  and  $a_0$ . Additional constant loading tests were therefore performed at 105 N from  $a = 24$  to  $a = 30$  mm. Crack speed was recorded as a function of crack length in the same manner as in Section 4.2, and the results are plotted in Fig. 3. It appears that crack velocity, i.e. stress intensity factor, depends directly on the  $a/a_0$  ratio. Indeed,

for the same applied load 105 N,  $\log(V)$  versus  $\log(a/a_0)$  defines the same straight line for the two notch lengths (namely 10 and 21 mm). This confirms the choice of the  $K_I$  expression on the form of eqn (14), and also gives an insight into the important role of the unbroken ligament on the compressive side of the specimen. We believe that the unbroken ligament induces contact stresses that act to create an additional moment arm on the tensile side. These contact stresses are inoperative in the case of a notched specimen without a natural crack, where the theoretical value of  $K_I$  in the form of eqn (7) is relevant, but they increase with the unbroken ligament area during crack extension. This increase induces a modification of stress intensity factor which is accurately taken into account in eqn (14).

## 6 CONCLUSIONS

(1) A variation of  $K_I$  of about 20% with crack length has been observed in a 3Y-TZP in the so-called linear region of the double torsion specimen.

(2) A correction is proposed for the stress intensity factor determination. This correction, which takes into account the influence of the crack length, appears to be important for accurate  $V$ - $K_I$  law determination. Although this work was done on a 3Y-TZP ceramic, we believe that such a correction can be applied to other ceramic or non-ceramic materials. It should be noted that the exponent  $m/k$  in the corrected  $K_I$  expression is function of both material and specimen geometry.

(3) Variation of  $K_I$  in the range of crack length investigated is neither due to the change in the compliance formula, nor to a decrease in the ratio of crack surface area increment to crack length increment  $\partial A/\partial a$ . The correction function  $\phi$  which takes into account the variation of local stress intensity factor over the thickness does not lead to a sufficient correction of  $V$ - $K_I$  law. Renotching experiments provide important clues to the role of the unbroken ligament on the compressive side of the specimen. We believe that contact stresses play a significant role on the observed variation of  $K_I$ .

These arguments have to be further confirmed with other materials, particularly with glass or monocrystalline ceramics to avoid microstructural effects, and other polycrystalline ceramics with a good control of microstructure.

## ACKNOWLEDGEMENTS

The authors thank B. Calès and Céramiques Techniques Desmarquest (France) for supplying

the material and financial support, and S. S. Samad-dar for constructive comments on the manuscript.

## REFERENCES

1. KIES, J. A. & CLARK, A. B., In *Proc. 2nd International Conference on Fracture*, Brighton, April 1969, ed. Chapman and Hall, London, 1969, pp. 483–91.
2. OUTWATER, J. O., MURPHY, M. C., KUMBLE, R. G. & BERRY, J. T., In *Fracture toughness and slow-stable cracking*, ASTM STP 559, 1974, pp. 127–38.
3. FULLER, E. R., An evaluation of double torsion testing — analysis. In *Fracture Mechanics Applied to Brittle Materials*, Proc. 11th Symposium on Fracture Mechanics, Part II, ed. S. W. Freiman. ASTM STP 678, pp. 3–19.
4. PLEKTA, B. J., FULLER, E. R. & KOEPKE, B. G., An evaluation of double torsion testing — experimental. In *Fracture Mechanics Applied to Brittle Materials*, Proc. 11th Symposium on Fracture Mechanics, Part II, ed. S. W. Freiman. ASTM STP 678, pp. 19–38.
5. WILLIAMS, D. P. & EVANS A. G., A simple method for studying slow crack growth, *Journal of Testing and evaluation*, **1**(4) (1973) 264–70.
6. SHETTY, D. K., VIRKAR, A. V. & HARWARD, M. B., *J. Am. Ceram. Soc.* — Discussions and Notes, **62** (5–6) (1979) 307–9.
7. MCKINNEY, K. R. & SMITH, H. L., *J. Am. Ceram. Soc.*, **56** (1973) 30–2.
8. SHETTY, D. L. & VIRKAR, A. V., *J. Am. Ceram. Soc.*, **61** (1978) 93–4.
9. TRANTINA, G. G., *J. Am. Ceram. Soc.*, **60** (1977) 338–41.
10. EVANS, E. G., *J. Mater. Sci.*, **7**, (1972) 1137–46.
11. POLLET J. C. & BURNS, S. J., *J. Am. Ceram. Soc.* — Discussions and Notes, **62** (1979) 426–7.
12. LIU, S. Y. & CHEN, I. W., *J. Am. Ceram. Soc.*, **74**, (1991) 1206–16.
13. DRANSMANN, G. W., STEINBRECH, R. W., PAJARES, A., GUIBERTEAU, F., DOMINGUEZ-RODRIGUEZ, A. & HEUER, A. H., *J. Am. Ceram. Soc.*, **77** (1994) 1194–201.
41. WIEDERHORN, S. M., Subcritical crack growth in ceramics. In *Fracture Mechanics of Ceramics, Vol. 2, Microstructure, Material and Applications*, ed. R. C. Bradt, D. P. Hasselman & F. F. Lange. Plenum Press, New York 1974.